Crumbs homologue 1 is required for maintenance of photoreceptor cell polarization and adhesion during light exposure

Serge A. van de Pavert[1,*], Albena Kantardzhieva[1,*], Anna Malysheva[1], Jan Meuleman[1], Inge Versteeg[1], Christiaan Levelt[1], Jan Klooster[1], Sylvia Geiger[2], Mathias W. Seeliger[2], Penny Rashbass[3], Andre Le Bivic[4] and Jan Wijnholds[1,‡]

[1]The Netherlands Ophthalmic Research Institute, Royal Netherlands Academy of Arts and Sciences, Meibergdreef 47, 1105 BA Amsterdam, The Netherlands
[2]Retinal Electrodiagnostics Research Group, Department of Ophthalmology, University of Tübingen, Schleichstr. 12-16, 72076 Tübingen, Germany
[3]Centre for Developmental Genetics, Department of Biomedical Science, University of Sheffield, Western Bank, Sheffield, S10 2TN, UK
[4]Laboratoire de Neurogenèse et Morphogenèse au cours du Développement et chez l'Adulte (NMDA), UMR 6156 CNRS, IBDM, Université de la Méditerranée, Campus de Luminy, case 907, 13288 Marseille CEDEX 09, France

*These authors contributed equally
‡Author for correspondence (e-mail: j.wijnholds@ioi.knaw.nl)

Accepted 4 May 2004
Journal of Cell Science 117, 4169-4177 Published by The Company of Biologists 2004
doi:10.1242/jcs.01301

Summary

Loss of Crumbs homologue 1 (CRB1) function causes either the eye disease Leber congenital amaurosis or progressive retinitis pigmentosa, depending on the amount of residual CRB1 activity and the genetic background. Crb1 localizes specifically to the sub-apical region adjacent to the adherens junction complex at the outer limiting membrane in the retina. We show that it is associated here with multiple PDZ protein 1 (Mupp1), protein associated with Lin-7 (Pals1 or Mpp5) and Mpp4. We have produced *Crb1*$^{-/-}$ mice completely lacking any functional Crb1. Although the retinas are initially normal, by 3-9 months the *Crb1*$^{-/-}$ retinas develop localized lesions where the integrity of the outer limiting membrane is lost and giant half rosettes are formed. After delamination of the photoreceptor layer, neuronal cell death occurs in the inner and outer nuclear layers of the retina. On moderate exposure to light for 3 days at 3 months of age, the number of severe focal retinal lesions significantly increases in the *Crb1*$^{-/-}$ retina. Crb2, Crb3 and Crb1 interacting proteins remain localized to the sub-apical region and therefore are not sufficient to maintain cell adhesion during light exposure in *Crb1*$^{-/-}$ retinas. Thus we propose that during light exposure Crb1 is essential to maintain, but not assemble, adherens junctions between photoreceptors and Müller glia cells and prevents retinal disorganization and dystrophy. Hence, light may be an influential factor in the development of the corresponding human diseases.

Supplemental data available online

Key words: Leber congenital amaurosis, Light induced degeneration, Cell polarity, Cell adhesion, Subapical region, Adherens junction

Introduction

Mutations causing amino acid substitutions in the human Crumbs homologue 1 (*CRB1*) gene, the human homologue of *Drosophila Crumbs*, can lead to Leber congenital amaurosis (LCA), classic and retinitis pigmentosa type 12, and retinitis pigmentosa with Coats-like exudative vasculopathy (Cremers et al., 2002; den Hollander et al., 1999; van Soest et al., 1999), whereas all known null mutations lead to LCA. LCA is a group of inherited severe retinal diseases characterized by loss of vision within one year after birth. It accounts for at least 5% of all retinal dystrophies and is one of the main causes of blindness in children (Cremers et al., 2002). Mutations in six genes were identified that together account for approximately 50% of all LCA patients. CRB1 accounts for 9-13.5% of these cases (Cremers et al., 2002). The CRB1 protein contains 19 epidermal growth factor-like domains, three laminin A globular-like domains, a transmembrane domain and a 37 amino acid cytoplasmic tail with an C-terminal ERLI motif (den Hollander et al., 1999; Tepass et al., 1990).

In the retina, photoreceptor cells (PRCs) transform the incoming light to a signal that is processed subsequently by other neurons in the retina and brain. The PRCs are packed together, with processes of Müller glia cells (MGCs) for structural and metabolic support, in the retinal outer nuclear layer (ONL). The establishment and maintenance of apical-basal polarization and cell adhesion is crucial for the PRCs. At the apical site of the ONL, an adhesion belt, named the outer limiting membrane (OLM), contains specialized adherens junctions (AJs), which are present between the PRCs and MGCs. The AJs consist of multi-protein complexes and are linked to the cell skeleton for cell shape (Tepass, 2002).

Crumbs, a transmembrane protein, is associated with the formation of adherens junctions between cells in *Drosophila* (Grawe et al., 1996; Tepass, 1996). It localizes at a specialized region apical to the AJs, the subapical region (SAR) (Pellikka et al., 2002; Tepass, 1996), and is an essential component of the intracellular scaffold for the assembly of the protein complex at the AJ (Bachmann et al., 2001; Klebes and Knust,

2000; Pellikka et al., 2002). Crumbs is important in regulating the length of the stalk-membrane in PRCs and in preventing light-induced PRC degeneration (Izaddoost et al., 2002; Johnson et al., 2002; Pellikka et al., 2002). Also, Crumbs-interacting proteins are essential for the correct positioning and the integrity of the AJ for epithelial cell polarity and during PRC morphogenesis. Stardust (Sdt) binds to the C-terminal ERLI motif of Crumbs and deletion of this motif results in complete abolition of interaction between Sdt and Crumbs. Sdt loss of function results in multi-layered epithelia and tissue disintegration (Bachmann et al., 2001; Grawe et al., 1996; Hong et al., 2001). Another Crumbs interacting partner in *Drosophila* is Pals1 associated tight junction protein (dPATJ; formerly known as Discs lost), which does not play an essential role in epithelial cell polarity or viability (Klebes and Knust, 2000; Lemmers et al., 2002; Pielage et al., 2003). Upon overexpression of *CRB1*, in polarized epithelial cells, CRB1 associates with tight junctions (Roh and Margolis, 2003). In the tight junctions it co-localizes with protein associated with Lin-7 (PALS1 or MPP5), which is the homologue of Sdt, and with Pals1 associated tight junction protein (PATJ) (Hurd et al., 2003; Lemmers et al., 2002).

Although *Drosophila* Crumbs is required for polarity and adhesion in embryonic epithelia and for stalk membrane morphogenesis in PRCs (Izaddoost et al., 2002; Johnson et al., 2002; Klebes and Knust, 2000; Knust and Bossinger, 2002; Pellikka et al., 2002), the role of mammalian Crb1 in retinal dystrophies is still unclear (den Hollander et al., 1999; den Hollander et al., 2002). A clue came from a natural Crb1 mutant mouse, retinal degeneration 8 (*rd8*), which produces a secreted truncated Crb1 protein (Crb1-rd8) of 1207 amino acids that lacks the single transmembrane and the intracellular domain. The *rd8* mouse developed irregularities at the outer limiting membrane and loss of PRCs (Mehalow et al., 2003).

We have been able, by inactivating both alleles of the *Crb1* gene, to produce a complete null and to examine the physiological role of Crb1 in the mammalian retina. Moreover, the localization of other components of the scaffolding complex was examined in vivo. We found that Crb1 has a central role in the scaffolding complex and is required for maintaining a single, organized layer of PRCs during light exposure. In its absence the adhesion between PRCs and MGCs is temporarily lost resulting in dramatic structural and functional changes.

Materials and Methods

Generation of *Crb1*$^{-/-}$ mice

Gene targeting was performed as described previously (Wijnholds et al., 1997). In short, a characterized 194 bp mouse *Crb1* cDNA fragment encompassing a 5′-noncoding region and exon 1 encoding the translation start site and transmembrane signal peptide of *Crb1* was used to screen an EMBL3 genomic 129/Ola DNA phage library. A targeting vector was constructed by assembling a 5.6 kb *Bam*HI 5′ *Crb1* genomic fragment, a hygromycin resistance gene driven by the mouse phosphoglycerate kinase promoter, and a 4.9 kb *Bgl*II 3′ fragment of the *Crb1* gene. Correct targeting deleted 2.9 kb of *Crb1* sequence containing the upstream promoter region, exon 1 encoding the start of the Crb1 protein, and part of intron 1. Two ES clones with normal karyotype were injected into C57BL/6 mouse blastocysts. The homozygous as well as the wild-type mouse stocks were maintained as a cross of C57Bl/6 and 129/Ola (50%/50%), and kept in a 12 hours dark/12 hours dimmed light cycle (100 lux). For multiplex-PCR genotype analysis, we detected the wild-type *Crb1* allele using a sense primer JW1 (5′-CTGGGAGGGGTGGGACAG-3′) and an antisense primer JW105 (5′-AAAACCTGGACCAGAAGCGC-3′). These primer pairs amplify a 351-bp fragment from wild-type Crb1. The mutant allele was amplified using antisense primer JW105 and a sense primer JW123 (5′-GCTGTGTAGAAGTACTCGCCG-3′). All animals were treated according to guidelines established at the institutions in which the experiments were performed.

Morphological and immunohistochemical analysis

Affinity purified rabbit polyclonal antibodies raised against the C-terminal 36 amino acid peptide of human CRB1 (AK7) and the C-terminal 19 aa peptide of mouse Crb1 (AK2), antibodies raised against the C-terminal WNLMPPPAMERLI amino acids (EP13), the extracellular GPAWEGPRCEIRAD amino acids (EP14) and cytoplasmic CARLEMDSVLKVPPEE amino acid domains of human CRB2, and internal 15 amino acids peptides (KCVEADEETFESEEL) conserved between human membrane palmitoylated protein 4 (MPP4) and mouse Mpp4 (AK4), were generated and purified following standard procedures.

After fixation with 4% paraformaldehyde in PBS the mouse eye-cups were cryo-protected with sucrose. Snap-frozen human eyes were obtained from the Cornea Bank Amsterdam, with a post mortum period of 8-24 hours. Cryosections (7 μm) were rehydrated in PB and blocked for 1 hour using 10% goat or donkey serum, 0.4% Triton X-100 and 0.1% BSA in PB. Tissues for anti-Pals1 (protein associated with Lin-7) staining were blocked and permeabilized in 10% goat or donkey serum, 1% SDS and 0.1% BSA in PBS for 1 hour. Primary antibodies were diluted in 0.3% goat or donkey serum, 0.4% Triton X-100 and 0.1% BSA in PB and incubated for 16 hours. Secondary antibodies were diluted in 0.1% goat or donkey serum in PB and incubated for 1 hour at room temperature. For details on antibodies and concentrations, see Supplementary data (http://jcs.biologists.org/supplemental/). Sections were imaged on a Zeiss 501 confocal laser scanning microscope. Confocal images were processed with the Zeiss LSM image browser v3.2 and figures were assembled in Adobe Photoshop v7.0. Details on electron microscopy are available on request.

Light exposure and analysis of retinal damage

Prior to the start of the light exposure, all mice were maintained in a 12 hours dark/12 hours dimmed light (100 lux) cycle. After a 12-hour dark period mice were continuously exposed for 72 hours to 3000 lux of diffuse white fluorescent light (TLD-18W/33 tubes, Philips; 350-700 nm) without pupillary dilation. A correlation between codon 450 polymorphism in *Rpe65* and light-sensitivity (Wenzel et al., 2001) in *Crb1*$^{-/-}$ or wild-type retinas was excluded (for details, see Supplemental data, http://jcs.biologists.org/supplemental/). Immediately after light exposure, the eyes were orientated and thereafter enucleated, fixed either for cryosectioning or for 3 μm sectioning in Technovit 7100 (Kultzer, Wehrheim, Germany). In the latter, the whole retina was examined for protrusions and ingressions. Statistical analysis was performed using the Mann-Whitney test. Significance was accepted if $P<0.05$. For apoptosis analysis, the rhodamine in situ cell death detection kit (Roche, Mijdrecht, The Netherlands), a TdT-mediated dUTP nick-end labeling (TUNEL) assay, was used on 7 μm cryosections, according to the manufacturer's suggested protocol, and included 1:5 dilution of the labelling mix. As positive control, sections treated with DNAse were used according to manufacturer's protocol. Images were obtained with a Leica DMRD microscope and DC350F digital camera (Leica, Rijswijk, The Netherlands).

Immunoprecipitation experiments

Retinas were isolated from 3-month-old wild-type and *Crb1*$^{-/-}$ mice

and homogenized in lysis buffer (1% Triton X-100, 150 mM NaCl, 1 mM EDTA, 1 mM PMSF, 1 mM Na_3VO_4, 50 mM Tris-HCl, pH 7.4 containing a complete protease inhibitor cocktail). Crude lysates were cleared by centrifugation (10,000 ***g*** for 15 minutes at 4°C) and were used for immunoprecipitation with AK2. Membrane fractions were prepared by homogenization of retinas in extraction buffer (10 mM NaCl, 3 mM $MgCl_2$, 1 mM DTT, 1 mM PMSF, 1 mM Na_3VO_4, 10 mM Hepes, pH 7.9 supplemented with a complete protease inhibitors cocktail) and subsequent differential centrifugation. Membrane fractions were resuspended in lysis buffer and cleared by centrifugation, the supernatants were used for immunoprecipitation with monoclonal anti- multiple PDZ domain protein 1 (Mupp1; Transduction Laboratories, Alphen aan de Rijn, The Netherlands). As a control, mouse IgGs (Sigma) were used to perform immunoprecipitation. The precipitated proteins were washed four times with lysis buffer, eluted with sample buffer and analyzed by western blotting.

Electroretinography and scanning-laser ophthalmoscopy

Electroretinography

ERGs and SLOs were obtained according to previously reported procedures (Seeliger et al., 2001). Briefly, following dark adaptation overnight, mice were anesthetized with ketamine (66.7 mg/kg) and xylazine (11.7 mg/kg), and the pupils were dilated. The ERG equipment consisted of a Ganzfeld bowl, a DC amplifier, and a PC-based control and recording unit (Multiliner Vision; Jaeger-Toennies, Hoechberg, Germany). Band-pass filter cut-off frequencies were 0.1 and 3000 Hz. Single flash recordings were obtained both under dark-adapted (scotopic) and subsequently light-adapted (photopic) conditions. Light adaptation was achieved with a background illumination of 30 cd/m^2 starting 10 minutes before photopic recordings. Single flash stimulus intensities were increased from 10^{-4} cd*s/m^2 to 25 cd*s/m^2, divided into ten steps of 0.5 and 1 log cd*s/m^2. Ten responses were averaged with an inter-stimulus interval (ISI) of either 5 seconds or 17 seconds (for 1, 3, 10, 25 cd*s/m^2).

Scanning-laser ophthalmoscopy

Fundus imaging was performed with a HRA scanning-laser ophthalmoscope (SLO; Heidelberg Instruments, Heidelberg, Germany) that provides two Argon wavelengths (blue, 488 nm and green, 514.5 nm) and an infrared diode laser (690 nm) for fundus visualization. The confocal diaphragm of the SLO allows imaging of different planes of the posterior pole, ranging from the surface of the retina down to the retinal pigment epithelium (RPE) and the choroid. Different planes can be viewed by varying the focus by about ±20 diopters.

Results

The localization of proteins in the outer limiting membrane

The photoreceptor layer in the retina contains a structure called the OLM that contains AJs, a region of cell-cell adhesion between PRCs and MGCs. We examined the localization of mouse Crb1 with mammalian homologues of Crumbs-interacting proteins and other AJ and tight junction proteins in wild-type retinas. At the subapical region (SAR), adjacent to the AJ, we detected a number of proteins: Crb1 (Fig. 1A), F-actin (Fig. 1B), membrane-associated guanylate kinase (MAGUK) proteins (Bachmann et al., 2001; Hong et al., 2001) membrane palmitoylated protein 4 (Mpp4) (Stohr and Weber, 2001) (Fig. 1C) and Pals1 (Roh et al., 2002; Wei and Malicki, 2002) (Fig. 1D), the PSD95/Dlg/ZO-1 (PDZ) motif containing proteins multiple PDZ protein 1 (Mupp1) (Hamazaki et al., 2002) (Fig. 1E) and Patj (Lemmers et al., 2002; Roh et al., 2002) (Fig. 1F) as well as atypical protein kinase C (aPKC) (Fig. 1G). The Crb1 homologues Crb2 (Fig. 1H) and Crb3 (Makarova et al., 2003) (Fig. 1I), co-localized with Crb1 to the SAR. The AJ contained β-catenin (Fig. 1A), N-cadherin, p120 (Paffenholz et al., 1999), ZO-1 and ZO-2 (Itoh et al., 1999) (data not shown).

Patj was also detected in the retinal pigment epithelium (RPE) (data not shown). Mpp4 localized strongly in the synaptic terminal of the photoreceptors in the outer plexiform layer (data not shown and Fig. 5F). CD44 localized in the apical villi of the MGCs, but did not co-localize with Crb1 in the SAR (Fig. 1J). Cdc42 was detected in a similar localization pattern as F-actin, in the inner segments and outer plexiform layer (OPL) (data not shown). Next to the Crumbs complex,

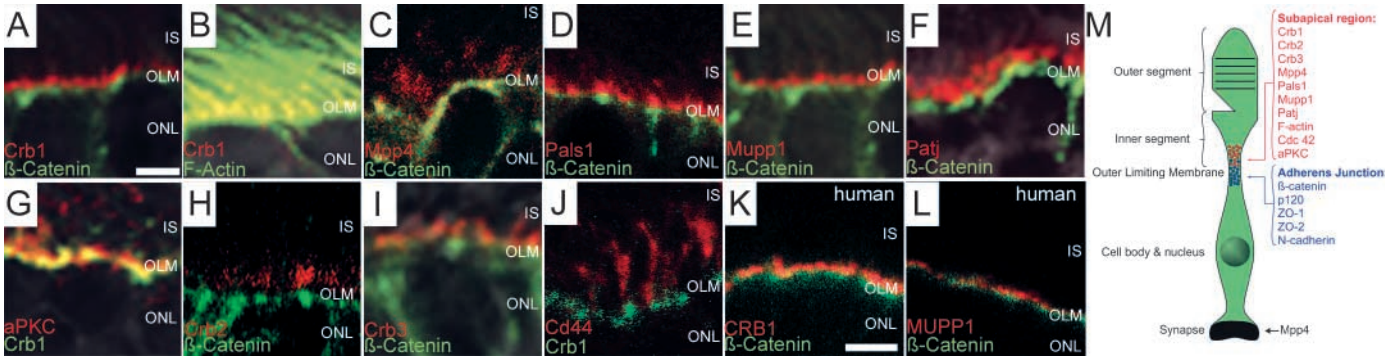

Fig. 1. Confocal images of 3-month-old wild-type mouse and human retinas. These images are high power insets of the OLM. (A) Crb1 is confined to the SAR, whereas β-catenin localized more basally at the AJ. (B) Crb1 localized at the basal part of the F-actin localization in the PRC inner segments. (C) Mpp4, (D) Pals1, (E) Mupp1 and (F) Patj localized at the SAR, compared to the location of β-catenin at the AJ. (G) aPKC co-localized with Crb1 to the SAR. (H-I) Crb2 and Crb3 localized to the SAR. A similar staining was detected in *Crb1*$^{-/-}$ retina. (J) CD44 localized in the MGC apical villi, but did not co-localize with Crb1 in the SAR. Par6, moesin or ZO-3 were not detected in the OLM (data not shown). Claudin-1 to -5 and occludin were not detected in the retina, but claudin-2 and occludin were detected in the retinal pigment epithelium (RPE). (K) CRB1 localized at the SAR of the human retina, apical to β-catenin in the AJ. (L) MUPP1 localized at the SAR of the human retina. (M) Schematic diagram of the localization for the different proteins at the SAR or AJ. Scale bar: 2.5 μm.

there are other complexes involved in establishing epithelial polarity, such as the Par3-Par6-aPKC-Cdc42 complex (Hurd et al., 2003). Components of this complex are known to interact with Crb family members and interacting proteins, e.g. Par6 has been shown to interact directly with Crb3 and Pals1 (Hurd et al., 2003; Lemmers et al., 2004). Of this complex, we detected aPKC and Cdc42 in the PRCs (Fig. 1G,M). This is the first study in mouse that defines the localization of several proteins at the OLM, such as Patj, Mupp1, Crb2, Crb3, Mpp4, aPKC and Cdc42. The localization of the homologues of these proteins, e.g. Crumbs in the SAR and Armadillo in the zonula adherens (ZA) in *Drosophila*, show remarkable similarities with our data in mouse (for a review, see Knust and Bossinger, 2002).

In the human retina, CRB1 and MUPP1 were detected at the SAR. The AJ was stained with a β-catenin antibody, while CRB1 and MUPP1 were located apical to this region (Fig. 1K,L), as in the mouse retina.

Binding partners of Crb1

To extend the co-localization studies further, we investigated which proteins associated together in the same complex. Immunoprecipitation of Mupp1 from retinal lysates demonstrated that endogenous Mupp1 interacted in PRCs in a protein-complex with Crb1, Pals1 and Mpp4 (Fig. 2). The antibody against Mupp1 efficiently co-precipitated Crb1, in agreement with co-localization of Crb1 with Mupp1 in the retina. Pals1 was efficiently co-precipitated as well. The Mpp4 protein was efficiently co-precipitated with Mupp1 from the outer limiting membrane given that most of the Mpp4 is localized at the outer plexiform layer (data not shown). The membrane-associated protein Patj was not detected in the Mupp1 precipitate (Fig. 2). In *Crb1*$^{-/-}$ retinas before the onset of retinal degeneration, the complex between Mupp1, Pals1 and Mpp4 formed in the absence of Crb1, indicating that Crb1 is not essential for this interaction (Fig. 2, first column). Pals1 was detected as a doublet (Hurd et al., 2003; Makarova et al., 2003). Both Pals1 proteins are present in the Mupp1 immunoprecipitate, with preference for the high molecular mass form. We conclude that in PRCs, Mupp1 is in complex with Pals1, Mpp4 and Crb1 and localized at the SAR.

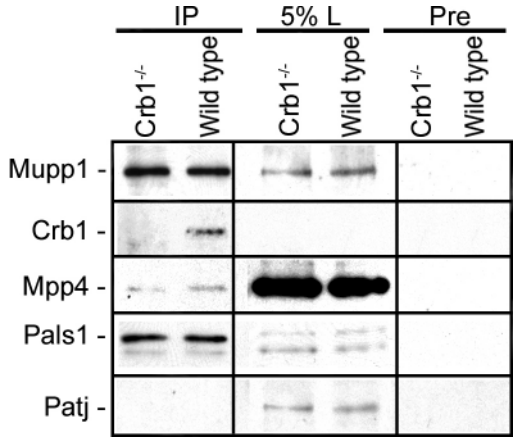

Fig. 2. Mupp1 immunoprecipitation (IP) co-precipitates Crb1, Mpp4 and Pals1. Crb1 was co-immunoprecipitated from retinal lysates of wild-type but not *Crb1*$^{-/-}$ mice. Patj was not found in the precipitated protein complex but was present only in the total retinal lysate (L). Anti-Pals1 detected a Pals1 doublet (Roh et al., 2002). In the control (Pre), mouse IgGs were used for immunoprecipitation.

Generation of *Crb1*$^{-/-}$ mice

We inactivated the murine *Crb1* gene (den Hollander et al., 2002) by deleting a 2.9 kb genomic DNA fragment in murine embryonic stem cells (Fig. 3A,B; see Materials and Methods). The deletion contained the upstream promoter of the gene and the first exon encoding the amino terminus of the Crb1 protein. The homozygous mice were healthy and fertile under normal conditions in the animal facilities. Antibodies directed against the carboxyl terminus of Crb1 did not detect Crb1 in retinal lysates of *Crb1*$^{-/-}$ mice (Fig. 3C). Using three different antibodies against Crb1, including that was described by Pelikka et al. (Pelikka et al., 2002), we observed localization of Crb1 specifically at the SAR in the inner segments of rods and cones of wild-type retinas (Fig. 3A), but not in the outer segments of the cones as previously described (Fig. 1A, Fig. 3D,E) (Pellikka et al., 2002). In *Crb1*$^{-/-}$ mice, Crb1 protein was not detected (Fig. 3F,G) indicating that the targeted allele is a true null.

Retinal morphology in *Crb1*$^{-/-}$ mice

In *Crb1*$^{-/-}$ mice, maintained in a 12 hours light (100 lux)/12 hours dark cycle, no abnormalities were detected in 2 or 3 weeks, or 2-month-old retinas (n=5 in each group). However by 3 months, *Crb1*$^{-/-}$ mice had developed small, but significant, regions of retinal degeneration that were never observed in wild-type controls (Fig. 4A-C). The OLM was ruptured by the protrusion of single or groups of PRC bodies into the interphotoreceptor space. Moreover, ingressed PRC bodies were also detected in the OPL and inner nuclear layer (INL) (Fig. 4A,B). A striking feature of the *Crb1*$^{-/-}$ phenotype was the presence of double PRC layers or half rosettes (Fig. 4C). The rosettes were immediately underneath the PRC layer and developed PRC inner segment membranes and an OLM. The number of PRCs in the upper and lower layers was approximately half the amount compared to the region immediately adjacent to the affected area, suggesting that the single PRC layer transformed into two layers without major loss of the PRCs. At this stage, except for the localized regions of retinal degeneration described in the next section (Fig. 5), the subcellular localizations of N-cadherin, β-catenin, p120, ZO-1, ZO-2, Patj, Mupp1, F-actin, Mpp4, Pals1, aPKC, Cdc42, Crb2 and Crb3 were similar to the wild-type (data not shown, Fig. 1). The gross ultra-structure of the AJ and the apical processes of MGCs, which extend for a short distance beyond the AJ, was normal when viewed by electron microscopy (Fig. S1, http://jcs.biologists.org/supplemental/). The outer segment membranes of wild-type and mutant mice were flat and well organized, and closely aligned with each other and the plasma membrane. Our results indicate that mouse Crb1 is not essential for the assembly of the SAR and AJ during PRC layer development but rather to maintain the correct position and integrity of the SAR and AJ. Since retinal degeneration occurred in the presence and normal subcellular localization of both Crb2 and Crb3 in *Crb1*$^{-/-}$ mice, it appeared that the

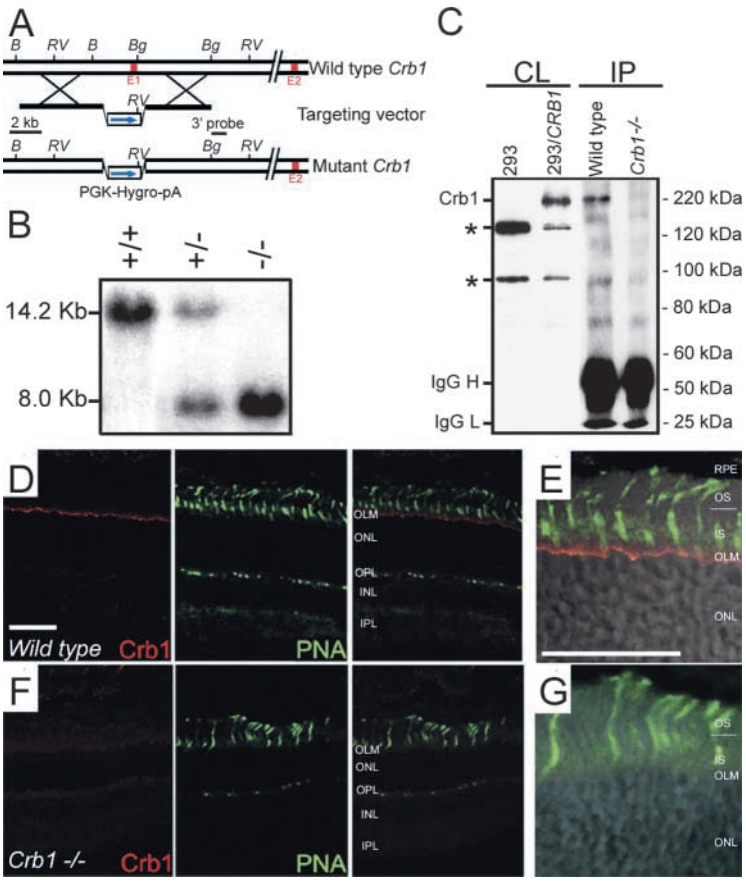

Fig. 3. Generation of *Crb1*$^{-/-}$ mice and confocal images of mouse retinas. (A) *Crb1* disrupted by insertion of the targeting vector. E1, exon 1; E2, Exon 2; pA, poly-adenylation signal; PGK, phosphoglycerate kinase promoter; *B*, *Bam*HI; *RV*, *Eco*RV; *Bg*, *Bgl*II. (B,C) Deletion of the exon encoding the N-terminal signal peptide prevents the production of Crb1 protein with C-terminal transmembrane and intracellular domains. (B) *Eco*RV Southern blot analysis using a 750 bp *Bgl*II-*Acc*I fragment probe in the 3′ flanking region. (C) Immunoprecipitation of Crb1, with AK7, from lysate of wild-type but not of the *Crb1*$^{-/-}$ retina. As positive control 293/CRB1 cell lysates were used. Crb1 was stained using AK2. Asterisks indicate cross-reacting bands with AK2 in 293 cells. (D-G) Localization of Crb1 (red) in the OLM and staining of cone segments and pedicles by peanut agglutinin (PNA; green) in the retinas of wild-type (D) and *Crb1*$^{-/-}$ (F) mice. Detail of the localization of Crb1 at the SAR for the wild-type (E) and *Crb1*$^{-/-}$ (G) retina. Scale bars: 30 μm.

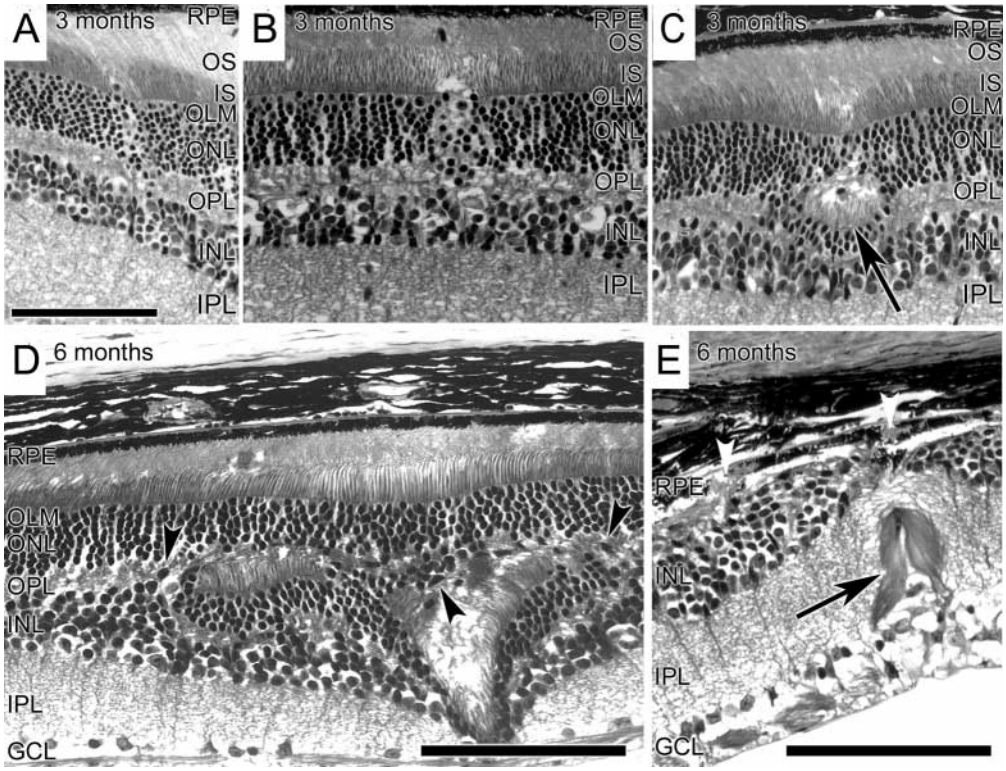

Fig. 4. Retinal phenotype of *Crb1*$^{-/-}$ mice exposed to cycled light (12 hours dark/12 hours 100 lux). (A-C) Different stages of degeneration in 3-month-old *Crb1*$^{-/-}$ retinas. (A) Start of degeneration in which some PRCs protrude through the OLM and ingress into the OPL. (B) More PRCs are involved in larger ingression areas and PRCs ingressed onto the INL. (C) Ingressed PRCs re-aggregate into half rosette structures, and form new inner segments and an OLM (arrow). (D,E) Morphology of 6-month-old *Crb1*$^{-/-}$ retinas. (D) Formation of a giant half rosette of PRCs with outgrown inner segments. Note the presence of cells from the INL, possibly MGC nuclei, close to the edges of and inside this structure (arrowheads). (E) Complete degeneration of the ONL, presence of ghost structure (arrow) and ingression of RPE into the retina (arrowheads). Scale bars: 100 μm.

presence of Crb2 and Crb3 is not sufficient to rescue the retinal degeneration phenotype.

Further indications for loss of PRC to MGC adhesion at foci in the retina were obtained by the analysis of 6-month old *Crb1*$^{-/-}$ mice. Large ectopic layers of PRCs formed a funnel-shaped layer, abutting the ganglion cell layer and inner limiting membrane (Fig. 4D). The ectopic layers of PRCs resembled giant half rosettes with outgrown inner segments and OLM. In the more severely affected *Crb1*$^{-/-}$ mutant retinas, ghost-like structures were detected, which may represent remnants of PRC rosettes that underwent cell death (Fig. 4E). In these areas, we detected loss of PRCs as well as cells from the INL, and degeneration of RPE, without significant loss of thickness of the retina (Fig. 4D). These results may explain in part the results by Jacobson et al., who observed thick retinas in LCA patients with *CRB1* mutation, compared to thin retinas in, for example, *RPE65* mutations (Jacobson et al., 2003).

Light exposure accelerates retinal degeneration in *Crb1*$^{-/-}$ mice

Mutations in *Drosophila crumbs* result in improper PRC morphogenesis and progressive light-induced PRC degeneration (Johnson et al., 2002). Since light could be one of the environmental factors causing the degenerations at foci in the *Crb1*$^{-/-}$ retinas, we exposed 3-month-old pigmented wild-type and *Crb1*$^{-/-}$ mice to continuous moderate white fluorescent light (3000 lux) for 3 days (Hao et al., 2002). In a representative experiment there was a significant increase in the number of degenerative areas in moderate light-exposed *Crb1*$^{-/-}$ retinas, compared to retinas exposed to cycled light (12 hours dark/12 hours 100 lux) (P<0.02, n=4) (Fig. 5A). The number of degenerative regions counted in the *Crb1*$^{-/-}$ retinas exposed to 3000 lux for 72 hours is probably an underestimate of the true number of foci affected, as we observed that several small foci appeared to fuse into larger abnormal regions as can be seen in Fig. 5B when compared to Fig. 4. Retinal degeneration started at several foci at the inferior temporal quadrant of the *Crb1*$^{-/-}$ retina, the area most exposed to light in the murine retina. In the moderate light-exposed *Crb1*$^{-/-}$ mice, retinal degeneration started as described for the 3- to 9-month *Crb1*$^{-/-}$ mice in cycled light (Fig. 5B). However, 3 days after moderate light exposure, PRCs apical to the rosettes lacked inner and outer segments (Fig. 5C). None of the moderate light-exposed wild-type retinas showed degenerative areas (n=10). Overall our results support the hypothesis that light is an environmental factor that enhances the onset of retinal degeneration in *Crb1*$^{-/-}$ retinas.

Light damage to the retina is detected early in MGCs, which respond by altering their protein levels and/or subcellular localization, e.g. by the upregulation and redistribution of intermediate filament proteins (Chen and Weber, 2002). We therefore used glial fibrillary acidic protein (GFAP) to stain intermediate filaments in MGCs. In *Crb1*$^{-/-}$ mice, ectopic GFAP staining correlated well with regions of detectable retinal degeneration. Strongly stained bundles of newly formed GFAP-positive intermediate filaments were detected through the INL and ONL. Moreover, MGCs extended further through the OLM into the interphotoreceptor space (Fig. 5D,E). In the degenerated areas, staining with markers for the OLM indicated disruptions at the SAR or AJ (Fig. 5F-J). Staining with markers for the OPL indicated losses of neuronal synapses at local regions (Fig. 5F,G). Remarkably, only a small number of TUNEL-positive cells were detected specifically at these sites of retinal degeneration in moderate light-exposed *Crb1*$^{-/-}$ mice (Fig. 5K,L), suggesting a delayed initiation of cell death after loss of PRC-MGC adhesion.

Electroretinography and fundus photography

The retinal function was examined by electroretinography. No loss of overall retinal function was detected in either the 3-, 6- (data not shown), or 9-month-old *Crb1*$^{-/-}$ mice exposed to cycled light, nor in 3-month-old *Crb1*$^{-/-}$ mice exposed for 72 hours to 3000 lux of light (Fig. S2, http://jcs.biologists.org/supplemental/). This is not surprising as the focal retinal degeneration observed is very localized, whilst the remainder of the retina appears grossly normal. In the 72-hour 3000 lux-exposed *Crb1*$^{-/-}$ mice, fundus photography revealed macroscopically visible retinal spots (Fig. 5M) that correlated with rosette structures and double PRC layers in the sections. In mice with rosette or pseudo-rosette formation but without double PRC layers, similar spots were detected (Akhmedov et al., 2000; Mehalow et al., 2003). No spots were observed on SLO in 3-, 6- or 9-month-old *Crb1*$^{-/-}$ retinas exposed to cycled light, most likely because the areas of retinal degeneration were very small.

Discussion

In this study, we present the generation and characterization of *Crb1*$^{-/-}$ knockout mice. We demonstrate that complete disruption of *Crb1* results in light-inducible retinal degeneration. The onset of the disease is due to transient loss of cell adhesion between PRCs and MGCs. When PRCs re-adhere, rosette structures and double PRC layers are formed. It has been demonstrated that MGCs rescue nearby PRCs from apoptosis and prolong their survival by the expression of growth factors (Harada et al., 2000). These MGC-derived growth factors might be essential in the transient rescue of PRCs in the ectopic rosette structures and double PRC layers in *Crb1*$^{-/-}$ retinas. Hence, Crb1 is not essential for the initial assembly of the AJs between PRCs and MGCs, but rather for the maintenance of the AJs during light exposure.

In most polarized vertebrate epithelial cells, tight junctions are located apical to the AJ. In the retina, the OLM harbours an AJ and a distinct region apical to the AJ, the SAR. We provide novel data on Crb1 co-localization with Mpp4, Cdc42, F-Actin, Patj, Mupp1, aPKC, Crb2 and Crb3 in the SAR. Localization of Pals1 in the SAR was also confirmed (Mehalow et al., 2003). Cell-cell contact in the OLM is not tight, since large molecules such as colloidal thorium and peroxidase (Feeney, 1973; Peyman et al., 1971) readily diffuse from the vitreous through the OLM, into the interphotoreceptor space. In accordance, claudins 1-5 were not detected at the SAR.

The complex of Crb1, Pals1 and Mpp4 with Mupp1 has not been demonstrated before in vivo. In cultured epithelial cells it was shown by Roh et al. (Roh et al., 2002; Roh et al., 2003) that PALS1 binds to CRB1 and that PALS1 binds to the L27-like domain in PATJ and MUPP1 (Roh et al., 2002; Roh and Margolis, 2003). MPP4, a family member of Pals1, also interacted with CRB1 when overproduced in 293 human

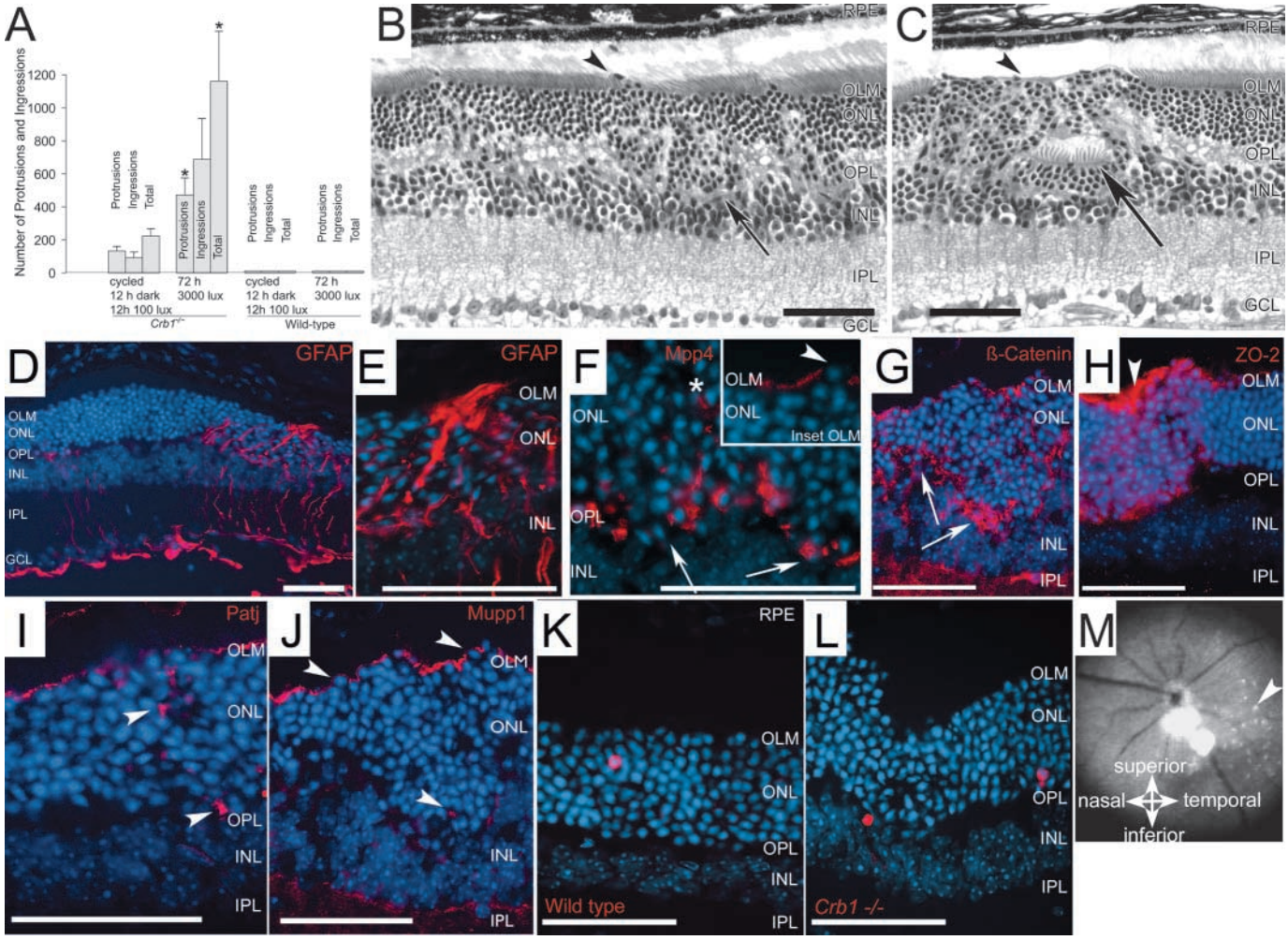

Fig. 5. Retinal phenotype of 3-month-old *Crb1*$^{-/-}$ mice exposed to 3000 lux for 72 hours. (A) Representative experiment with wild-type and *Crb1*$^{-/-}$ retinas indicating number of protrusions, ingressions and total amount in cycled light (12 hours dark/12 hours 100 lux) versus 72 hours of 3000 lux. Error bars represent s.e.m. Asterisks indicate statistical difference (P<0.02) between the groups exposed to cycled light and 72 hours of 3000 lux. (B) Numerous ingression areas through the OPL (arrow) and protrusions through a distorted OLM (arrowhead) in the *Crb1*$^{-/-}$ retina. (C) OLM present in rosette (arrow), no segments are present on the disorganized PRCs (arrowhead). (D-J) Fluorescence microscopy images of degenerated areas. Nuclei are stained with Hoechst (blue). Note that in unaffected areas, adjacent to the ingression areas, localization of the proteins is normal. GFAP localized near the inner limiting membrane, at the MGC end-feet and in horizontally radiating MGC rootlets in the OPL (data not shown) in wild-type mice exposed to both cycled light and 72 hours of 3000 lux. (E) Detail of D, strong staining of GFAP in the ONL and through OLM. (F) Areas of protrusions (arrowheads) and ingressions (arrows) where Mpp4 is lost at the OLM and OPL as well as mislocalized into the ONL (asterisk). (G) β-Catenin mislocalization throughout the ONL in ingression areas (arrows). (H) ZO-2 localization perturbed in a protrusion and ingression area. (I,J) Mislocalization and loss of Patj or Mupp1 in affected areas (arrowheads). (K) Apoptotic cells are rarely present in wild-type retinas. (L) Slightly increased apoptosis is apparent in *Crb1*$^{-/-}$ mice around ingression areas. Scale bars: 50 μm. (M) SLO image (514.5 nm) of a 3-month-old *Crb1*$^{-/-}$ mouse fundus after exposure for 72 hours to 3000 lux. The multiple dots (arrowhead) indicate areas of rosette formation in the inferior temporal quadrant of the retina. Scale bars: 50 μm.

embryonic kidney cells (A.K. and J.W., unpublished results). It is therefore probable that separate complexes of Crb1-Pals1-Mupp1 and Crb1-Mpp4-Mupp1 exist, or since MAGUK proteins may form heterodimers or homodimers (Nix et al., 2000), that complexes of Crb1-Pals1/Mpp4-Mupp1 are present in the PRCs. Conditions used for Patj immunoprecipitation were not optimal for the demonstration of a Patj-Pals1-Mpp4-Crb1 complex (data not shown). However, the interaction between Patj and Pals1 has been shown by others with overexpression in epithelial cell culture (Lemmers et al., 2002; Roh et al., 2002). Since Patj co-localizes with Crb1 and Mupp1 at the SAR, it is therefore conceivable that Crb1-Pals1/Mpp4-Patj complexes also exist.

The many different mutations in the human *CRB1* gene cause variable eye phenotypes, e.g. LCA, retinitis pigmentosa type 12, classic retinitis pigmentosa, and retinitis pigmentosa with Coats-like exudative vasculopathy. Full ablation of CRB1 function is likely to result in LCA (Cremers et al., 2002), whereas other amino acid substitutions in the extracellular domain of CRB1 are likely to result in different forms of retinitis pigmentosa. The same may be true for truncated CRB1 proteins lacking the transmembrane and cytosolic domains

(Cremers et al., 2002). Mehalow et al. (Mehalow et al., 2003) recently identified a mutation in the *Crb1* gene responsible for the *rd8* retinal degeneration phenotype. The *rd8* mutation is most probably not a null allele, but encodes an aberrant secreted truncated Crb1-rd8 protein of 1207 amino acids, of which 47 are novel amino acids. This aberrant protein lacks four of the 19 epidermal growth-factor domains and one of the three laminin A G-like domains (Mehalow et al., 2003). The production of Crb1-rd8 in combination with the lack of the native Crb1 protein causes retinal folds (pseudorosettes), very different from the double photoreceptor layers (giant half-rosettes) observed in the *Crb1*$^{-/-}$ mice. In old *rd8* mice the photoreceptor layer declines to a single row of PRCs. In contrast, in foci of *Crb1*$^{-/-}$ retinas, complete loss of PRCs and INL, as well as degeneration of RPE occurs after an initial transformation of single to double photoreceptor layers. The difference in phenotype could be the result of genetic background or residual Crb1 function in the Crb1-rd8 protein (Mehalow et al., 2003). Also, in the *rd8* mice many irregularly shaped spots are detectable as early as 3 weeks of age, whereas in the *Crb1*$^{-/-}$ mice these spots are sporadic at 3 months of age. An interesting difference is the localization of the spots, which were found in the inferior nasal quadrant of the fundus in *rd8* mice, but in the inferior temporal quadrant in *Crb1*$^{-/-}$ retina corresponding to the area most exposed to light. Furthermore, some similarities in phenotype are detected, such as discontinuous staining of β-catenin, N-cadherin or Pals1 at affected regions.

We propose that the *Crb1*$^{-/-}$ mouse is a model for those LCA patients completely lacking functional CRB1. Our data suggest that exposure to daylight accelerates retinal degeneration. Our results indicate that Crb1 is not essential for the assembly of the SAR and AJ during PRC layer development but rather for maintaining the correct position and integrity of the SAR and AJ. The carboxyl termini of murine Crb1 and Crb3 interact in vitro with the PDZ domain of Pals1 (Makarova et al., 2003; Roh et al., 2002). Redundant functions of Crb1, Crb2 and Crb3 in photoreceptors are not known but their co-localization at the SAR, the high similarity of their C termini, and interaction with Pals1 suggest a possible overlap or competition in function. Therefore, Crb3 could be involved, by interacting with Pals1-Patj/Mupp1, in the assembly of the SAR and AJ. Also the function and possible redundancy of Crb2, which is highly similar to Crb1, remains to be investigated.

It has been suggested that the mammalian CRB1 could have the same function as *Drosophila* Crumbs (Johnson et al., 2002; Pellikka et al., 2002). Our results show that, although there is some overlap, there are differences between mammalian CRB1 and *Drosophila* Crumbs. In *Drosophila* only one Crumbs protein is present, whereas in the mouse there may be redundant overlapping functions for Crb1, Crb2 and Crb3, the latter two with yet unknown physiological function(s). Crumbs regulates the length of the stalk membrane in the PRCs of *Drosophila*, a structure hypothesized to share function with inner segments of PRCs (Pellikka et al., 2002). However, the length of inner segments of mutant and wild-type mice did not differ (data not shown). Therefore, our data suggest that Crb1 does not regulate the length of the inner segments of PRCs, or that other proteins (e.g. Crb2 or Crb3) exert similar functions. Unlike the PRCs in the fruit fly (Izaddoost et al., 2002; Pellikka et al., 2002), loss of cell polarization and adhesion in *Crb1*$^{-/-}$ mice is transient as shown by newly formed layers of PRCs with an OLM. These data suggest possible overlap of functions for the Crb1 family members, and a central role for Crb1 as a component of the molecular scaffold that controls maintenance of the PRC AJ during exposure to light. These findings provide insight into PRC layer polarization and retinal degeneration, and they reveal that Crb1 protects PRCs against physiological stress induced by light. Since LCA develops early in life in humans, by the time the pathology of the retinas is examined, the retina has completely degenerated. One study (Jacobson et al., 2003), using optical coherence tomography in vivo on LCA patients until 50 years of age, indicated a change in morphology. However, the onset of the pathology and delamination of the PRC layer have not been described in LCA patients. Therefore, the *Crb1*$^{-/-}$ mouse model could be useful in obtaining more knowledge on the onset of LCA. Moreover, understanding the role of light in the onset of LCA, in patients with *CRB1* mutations, will assist in prevention of retinal dystrophy.

We thank C.A.A.M. Mol-Neefjes for excellent technical assistance; J. van der Vliet for immunizing rabbits; U. Tepass for anti-Crb1 (851); R. van der Neut for anti-CD44; M. Roh and B. Margolis for the anti-Crb3, anti-Pals1 and anti-Patj antibodies; T. van den Berg for light spectrum analysis; T. Gorgels for the light-experiment equipment; B. Nunes-Cardozo for assistance with the CLSM; The Cornea Bank Amsterdam for providing the donor eyes; A.A. Put for the artwork; S. Alexeeva, A. Bergen, P.T.V.M. de Jong and W. Kamphuis for discussions and critical reading of the manuscript. Support for this research was provided by the DFG (to M.W.S.), ZonMW-NWO (912-02-018) and EC grants (to J.W., A.L.B. and P.R. respectively) (QLG3-CT-2002-01266).

References

Akhmedov, N. B., Piriev, N. I., Chang, B., Rapoport, A. L., Hawes, N. L., Nishina, P. M., Nusinowitz, S., Heckenlively, J. R., Roderick, T. H., Kozak, C. A. et al. (2000). A deletion in a photoreceptor-specific nuclear receptor mRNA causes retinal degeneration in the rd7 mouse. *Proc. Natl. Acad. Sci. USA* **97**, 5551-5556.

Bachmann, A., Schneider, M., Theilenberg, E., Grawe, F. and Knust, E. (2001). Drosophila Stardust is a partner of Crumbs in the control of epithelial cell polarity. *Nature* **414**, 638-643.

Chen, H. and Weber, A. J. (2002). Expression of glial fibrillary acidic protein and glutamine synthetase by Muller cells after optic nerve damage and intravitreal application of brain-derived neurotrophic factor. *Glia* **38**, 115-125.

Cremers, F. P., van den Hurk, J. A. and den Hollander, A. I. (2002). Molecular genetics of Leber congenital amaurosis. *Human Mol. Genet.* **11**, 1169-1176.

den Hollander, A. I., ten Brink, J. B., de Kok, Y. J., van Soest, S., van den Born, L. I., van Driel, M. A., van de Pol, D. J., Payne, A. M., Bhattacharya, S. S., Kellner, U. et al. (1999). Mutations in a human homologue of Drosophila crumbs cause retinitis pigmentosa (RP12). *Nat. Genet.* **23**, 217-221.

den Hollander, A. I., Ghiani, M., de Kok, Y. J., Wijnholds, J., Ballabio, A., Cremers, F. P. and Broccoli, V. (2002). Isolation of Crb1, a mouse homologue of Drosophila crumbs, and analysis of its expression pattern in eye and brain. *Mech. Dev.* **110**, 203-207.

Feeney, L. (1973). The interphotoreceptor space. I. Postnatal ontogeny in mice and rats. *Dev. Biol.* **32**, 101-114.

Grawe, F., Wodarz, A., Lee, B., Knust, E. and Skaer, H. (1996). The Drosophila genes crumbs and stardust are involved in the biogenesis of adherens junctions. *Development* **122**, 951-959.

Hamazaki, Y., Itoh, M., Sasaki, H., Furuse, M. and Tsukita, S. (2002). Multi-PDZ domain protein 1 (MUPP1) is concentrated at tight junctions through its possible interaction with claudin-1 and junctional adhesion molecule. *J. Biol. Chem.* **277**, 455-461.

Hao, W., Wenzel, A., Obin, M. S., Chen, C. K., Brill, E., Krasnoperova, N. V., Eversole-Cire, P., Kleyner, Y., Taylor, A., Simon, M. I. et al. (2002). Evidence for two apoptotic pathways in light-induced retinal degeneration. *Nat. Genet.* **32**, 254-260.

Harada, T., Harada, C., Nakayama, N., Okuyama, S., Yoshida, K., Kohsaka, S., Matsuda, H. and Wada, K. (2000). Modification of glial-neuronal cell interactions prevents photoreceptor apoptosis during light-induced retinal degeneration. *Neuron* **26**, 533-541.

Hong, Y., Stronach, B., Perrimon, N., Jan, L. Y. and Jan, Y. N. (2001). Drosophila Stardust interacts with Crumbs to control polarity of epithelia but not neuroblasts. *Nature* **414**, 634-638.

Hurd, T. W., Gao, L., Roh, M. H., Macara, I. G. and Margolis, B. (2003). Direct interaction of two polarity complexes implicated in epithelial tight junction assembly. *Nat. Cell Biol.* **5**, 137-142.

Itoh, M., Morita, K. and Tsukita, S. (1999). Characterization of ZO-2 as a MAGUK family member associated with tight as well as adherens junctions with a binding affinity to occludin and alpha catenin. *J. Biol. Chem.* **274**, 5981-5986.

Izaddoost, S., Nam, S. C., Bhat, M. A., Bellen, H. J. and Choi, K. W. (2002). Drosophila Crumbs is a positional cue in photoreceptor adherens junctions and rhabdomeres. *Nature* **416**, 178-183.

Jacobson, S. G., Cideciyan, A. V., Aleman, T. S., Pianta, M. J., Sumaroka, A., Schwartz, S. B., Smilko, E. E., Milam, A. H., Sheffield, V. C. and Stone, E. M. (2003). Crumbs homolog 1 (CRB1) mutations result in a thick human retina with abnormal lamination. *Human Mol. Genet.* **12**, 1073-1078.

Johnson, K., Grawe, F., Grzeschik, N. and Knust, E. (2002). Drosophila crumbs is required to inhibit light-induced photoreceptor degeneration. *Curr. Biol.* **12**, 1675-1680.

Klebes, A. and Knust, E. (2000). A conserved motif in Crumbs is required for E-cadherin localization and zonula adherens formation in Drosophila. *Curr. Biol.* **10**, 76-85.

Knust, E. and Bossinger, O. (2002). Composition and formation of intercellular junctions in epithelial cells. *Science* **298**, 1955-1959.

Lemmers, C., Medina, E., Delgrossi, M. H., Michel, D., Arsanto, J. P. and le Bivic, A. (2002). hINADl/PATJ, a homolog of discs lost, interacts with crumbs and localizes to tight junctions in human epithelial cells. *J. Biol. Chem.* **277**, 25408-25415.

Lemmers, C., Michel, D., Lane-Guermonprez, L., Delgrossi, M. H., Medina, E., Arsanto, J. P. and le Bivic, A. (2004). CRB3 binds directly to Par6 and regulates the morphogenesis of the tight junctions in mammalian epithelial cells. *Mol. Biol. Cell* **15**, 1324-1333.

Makarova, O., Roh, M. H., Liu, C. J., Laurinec, S. and Margolis, B. (2003). Mammalian Crumbs3 is a small transmembrane protein linked to protein associated with Lin-7 (Pals1). *Gene* **302**, 21-29.

Mehalow, A. K., Kameya, S., Smith, R. S., Hawes, N. L., Denegre, J. M., Young, J. A., Bechtold, L., Haider, N. B., Tepass, U., Heckenlively, J. R. et al. (2003). CRB1 is essential for external limiting membrane integrity and photoreceptor morphogenesis in the mammalian retina. *Human Mol. Genet.* **12**, 2179-2189.

Nix, S. L., Chishti, A. H., Anderson, J. M. and Walther, Z. (2000). hCASK and hDlg associate in epithelia, and their src homology 3 and guanylate kinase domains participate in both intramolecular and intermolecular interactions. *J. Biol. Chem.* **275**, 41192-41200.

Paffenholz, R., Kuhn, C., Grund, C., Stehr, S. and Franke, W. W. (1999). The arm-repeat protein NPRAP (neurojungin) is a constituent of the plaques of the outer limiting zone in the retina, defining a novel type of adhering junction. *Exp. Cell Res.* **250**, 452-464.

Pellikka, M., Tanentzapf, G., Pinto, M., Smith, C., McGlade, C. J., Ready, D. F. and Tepass, U. (2002). Crumbs, the Drosophila homologue of human CRB1/RP12, is essential for photoreceptor morphogenesis. *Nature* **416**, 143-149.

Peyman, G. A., Spitznas, M. and Straatsma, B. R. (1971). Peroxidase diffusion in the normal and photocoagulated retina. *Invest. Ophthalmol.* **10**, 181-189.

Pielage, J., Stork, T., Bunse, I. and Klambt, C. (2003). The Drosophila cell survival gene discs lost encodes a cytoplasmic Codanin-1-like protein, not a homolog of tight junction PDZ protein Patj. *Dev. Cell* **5**, 841-851.

Roh, M. H. and Margolis, B. (2003). Composition and function of PDZ protein complexes during cell polarization. *Am. J. Physiol. Renal Physiol.* **285**, F377-F387.

Roh, M. H., Makarova, O., Liu, C. J., Shin, K., Lee, S., Laurinec, S., Goyal, M., Wiggins, R. and Margolis, B. (2002). The Maguk protein, Pals1, functions as an adapter, linking mammalian homologues of Crumbs and Discs Lost. *J. Cell Biol.* **157**, 161-172.

Seeliger, M. W., Grimm, C., Stahlberg, F., Friedburg, C., Jaissle, G., Zrenner, E., Guo, H., Reme, C. E., Humphries, P., Hofmann, F. et al. (2001). New views on RPE65 deficiency, the rod system is the source of vision in a mouse model of Leber congenital amaurosis. *Nat. Genet.* **29**, 70-74.

Stohr, H. and Weber, B. H. (2001). Cloning and characterization of the human retina-specific gene MPP4, a novel member of the p55 subfamily of MAGUK proteins. *Genomics* **74**, 377-384.

Tepass, U. (1996). Crumbs, a component of the apical membrane, is required for zonula adherens formation in primary epithelia of Drosophila. *Dev. Biol.* **177**, 217-225.

Tepass, U. (2002). Adherens junctions, new insight into assembly, modulation and function. *BioEssays* **24**, 690-695.

Tepass, U., Theres, C. and Knust, E. (1990). Crumbs encodes an EGF-like protein expressed on apical membranes of Drosophila epithelial cells and required for organization of epithelia. *Cell* **61**, 787-799.

van Soest, S., van Rossem, M. J., Heckenlively, J. R., van den Born, L. I., de Meulemeester, T. M., Vliex, S., de Jong, P. T., Bleeker-Wagemakers, E. M., Westerveld, A. and Bergen, A. A. (1999). Integrated genetic and physical map of the 1q31–q32.1 region, encompassing the RP12 locus, the F13B and HF1 genes, and the EEF1AL11 and RPL30 pseudogenes. *Cytogenet. Cell Genet.* **84**, 22-27.

Wei, X. and Malicki, J. (2002). nagie oko, encoding a MAGUK-family protein, is essential for cellular patterning of the retina. *Nat. Genet.* **31**, 150-157.

Wenzel, A., Reme, C. E., Williams, T. P., Hafezi, F. and Grimm, C. (2001). The Rpe65 Leu450Met variation increases retinal resistance against light-induced degeneration by slowing rhodopsin regeneration. *J. Neurosci.* **21**, 53-58.

Wijnholds, J., Evers, R., van Leusden, M. R., Mol, C. A., Zaman, G. J., Mayer, U., Beijnen, J. H., van der Valk, M., Krimpenfort, P. and Borst, P. (1997). Increased sensitivity to anticancer drugs and decreased inflammatory response in mice lacking the multidrug resistance-associated protein. *Nat. Med.* **3**, 1275-1279.